Perfectly Matched Layer-Absorbing Boundary Condition for Left-Handed Materials

X. T. Dong, *Member, IEEE*, X. S. Rao, Y. B. Gan, *Senior Member, IEEE*, B. Guo, and W. Y. Yin, *Senior Member, IEEE*

***Abstract*—The perfectly matched layer (PML) absorbing boundary condition (ABC) is extended to truncate the boundary of left-handed materials in the Finite-Difference Time-Domain (FDTD) simulation. The unixial material parameters are given in the frequency domain, and discretized in the FDTD update procedure by means of the Z-Transform technique. The effectiveness of the PML is demonstrated by numerical results.**

***Index Terms*—Finite-difference time-domain (FDTD) method, left-handed material, perfectly matched layer.**

I. Introduction

LEFT-HANDED materials (LHMs), a class of metamaterials with negative permittivity and permeability, have attracted much attention due to their unique electromagnetic properties and potential applications [1], [2]. However, hot debates concerning their properties still remain [3], [4]. In order to verify the predicted EM properties of the LHMs, the importance of full-wave numerical simulations has been highlighted, while the available experimental data are very limited. The finite-difference time-domain (FDTD) method, one of the most important full-wave numerical methods, has been employed for this purpose and found to be successful [5], [6].

In the FDTD simulation, absorbing boundary conditions (ABCs) are needed to truncate the computation domain without reflection. Among them, the perfectly matched layer (PML) introduced by Berenger [7] has been the most popular. However, Berenger's PML was based on the split field equations that involved modification of Maxwell's equations. Sacks [8] approached the PML in an alternative way by using a layer of uniaxial lossy medium, avoiding the field splitting. Based on his work, Gedney demonstrated the FDTD implementation and the effectiveness of the uniaxial PML in [9] and [10], for free space and highly dispersive medium, respectively. Unfortunately, although the permittivity and permeability of the LHMs are also frequency-dependent, the PML shown in [10] cannot be used at the boundary of LHMs without modification, as found in Section II.

In this paper, Gedney's PML is modified for use on LHMs. First, the material parameters of the uniaxial PML are given. Next, the Z-Transform method [11] is applied to implement the frequency-dependent material property in the FDTD lattice. Numerical results demonstrated the effectiveness of the PML.

Manuscript received June 4, 2003; revised October 27, 2003. The review of this letter was arranged by Associate Editor S. Kawasaki.

The authors are with the National University of Singapore, Singapore 119260.

Digital Object Identifier 10.1109/LMWC.2004.827104

II. PML for LHM

The uniaxial material parameter of the PML is given by [8]–[10]

$$\frac{\overline{\overline{\varepsilon}}(\omega)}{\varepsilon_0\varepsilon_r(\omega)} = \frac{\overline{\overline{\mu}}(\omega)}{\mu_0\mu_r(\omega)} = \overline{\overline{\Lambda}} = \begin{pmatrix} a_\omega & & \\ & b_\omega & \\ & & c_\omega \end{pmatrix} \tag{1}$$

where $\varepsilon_r(\omega)$ and $\mu_r(\omega)$ are the permittivity and permeability of the background LHMs. To provide a nonreflective interface (normal to the z-axis), $a_\omega = b_\omega = 1/c_\omega$ must be satisfied. In [10], by assuming $a_\omega = \kappa_z + (\sigma_z/j\omega\varepsilon_0)$, $k_z \geq 1$, $\sigma_z \geq 0$, the PML works well for highly dispersive and lossy material. However, it fails when the background medium is a LHM. This can be understood as follows.

Consider a plane wave $E_x = E_0 e^{j\omega t - jkz}$, $H_y = H_0 e^{j\omega t - jkz}$, propagating along the z-axis. The material parameters in the PML are given by

$$\varepsilon_{xx} = \varepsilon_0\varepsilon_r(\omega)\kappa_z + \varepsilon_r(\omega)\frac{\sigma_z}{j\omega} \tag{2}$$

$$\mu_{yy} = \mu_0\mu_r(\omega)\kappa_z + \mu_0\mu_r(\omega)\frac{\sigma_z}{j\omega\varepsilon_0}. \tag{3}$$

At certain frequencies where both ε_r and μ_r are negative, the imaginary part of ε_{xx} and μ_{yy} will become positive. Therefore, the fields will be amplified, rather than attenuated in the PML region. On the other hand, we cannot just change the sign of σ_z, because the material permittivity and permeability differ with frequency and are not always negative in the whole frequency range.

Here, we modify the PML permittivity as follows:

$$\varepsilon_{xx} = \varepsilon_0\varepsilon_r(\omega)\kappa_z + \frac{\sigma_z}{j\omega}. \tag{4}$$

To maintain matched impedance between the PML and background medium, the permeability of PML should be

$$\mu_{yy} = \mu_0\mu_r(\omega)\kappa_z + \frac{\mu_0\mu_r(\omega)\sigma_z}{j\omega\varepsilon_0\varepsilon_r(\omega)}. \tag{5}$$

This equals to set $a_\omega = \kappa_z + (\sigma_z/j\omega\varepsilon_0\varepsilon_r(\omega))$ in (1). Such a PML can attenuate the electric and magnetic fields whenever $\varepsilon_r(\omega)$ and $\mu_r(\omega)$ and are negative or positive.

III. FDTD Discretization

The next step is to discretize the PML parameters into Yee's grid. It is convenient to use the D-B form in the FDTD lattice,

and update the E and H using frequency domain constitutive relation, via the Z-transform method [11]. The main idea of the Z-transform is to introduce $j\omega \Rightarrow (2/\Delta t)(1-z^{-1}/1+z^{-1})$ into the constitutive relation, where the z^{-1} operator can be interpreted as a delay operator, $z^{-1}F(z) \leftrightarrow F^{n-1}$. Thus, the field components can be written in a difference form as

$$E_x^{n+1} = \sum_{m=0}^{M} b_m D_x^{n-m+1} - \sum_{m=1}^{M} a_m E_x^{n-m+1} \tag{7}$$

$$H_y^{n+1} = \sum_{m=0}^{M} d_m B_y^{n-m+1} - \sum_{m=1}^{M} c_m H_y^{n-m+1}. \tag{8}$$

The coefficients $a_m \sim d_m$ are related to the medium parameters and the time step Δt. As an example, consider the commonly used permittivity and permeability for describing a LHM [5], [6]

$$\varepsilon_r(\omega) = 1 - \frac{\omega_{pe}^2}{\omega^2 - j\omega\Gamma_e} \tag{9}$$

$$\mu_r(\omega) = 1 - \frac{\omega_{pm}^2}{\omega^2 - j\omega\Gamma_m} \tag{10}$$

the coefficients $a_m \sim d_m$ are shown in the Appendix. The update coefficients inside the LHM can be calculated using the same equations by substituting and $\kappa_z = 1$ and $\sigma_z = 0$.

IV. Numerical Results and Discussions

To validate the efficiency of the PML termination, we show some numerical examples. Consider a Gaussian pulse $g(t) = e^{-(t-\tau)^2/t_0^2}$ propagating through the LHM along z direction, where $t_0 = 3 \times 10^{-11}$ s, $\tau = 1.2 \times 10^{-10}$ s. The FDTD cells are given by $\Delta z = 1$ mm and $\Delta t = \Delta z/C$. Note that the half-bandwidth of the incident pulse is about 16.67 GHz, the ratio of the wavelength to the grid cell size is $\lambda_0/\Delta z = 18$. The total number of FDTD cells is 100, with 10 cells of PML. Within the PML, the conductivity was scaled using the polynomial scaling [9], [10]. The electric field is recorded as E_{PML} at $z_1 = 20\Delta z$. A reference solution based on an extended lattice is also computed, recorded as E_{ref}. The relative error is defined as

$$\text{Reflection Error (dB)} = 20 \times \log_{10}\left(\frac{|E_{PML} - E_{\text{ref}}|}{|E_{\max}|}\right) \tag{11}$$

where $E_{\max}$ is the maximum value of the propagated electric field.

The simulation is done on a matched LHM, with $\omega_{pe} = \omega_{pm} = 3\pi \times 10^9$ rad/s, $\Gamma_e = \Gamma_m = 9 \times 10^7$ rad/s and an unmatched LHM, with $\omega_{pe} = 3\pi \times 10^9$ rad/s, $\omega_{pm} = 8\pi \times 10^9$ rad/s. Fig. 1 shows the reflection error as a function of time. It is found that for the matched material, the reflection error is about $-160 \sim -130$ dB. However, for the unmatched material, the time domain reflection error is about $-80 \sim -60$ dB.

In Fig. 2, the reflection error is shown as a function of frequency. Two sharp peaks are found in the unmatched case, corresponding to the two material frequencies, respectively. Away from this region, the error is below -90 dB. In contrast, the reflection error is better than -120 dB for the matched PML.

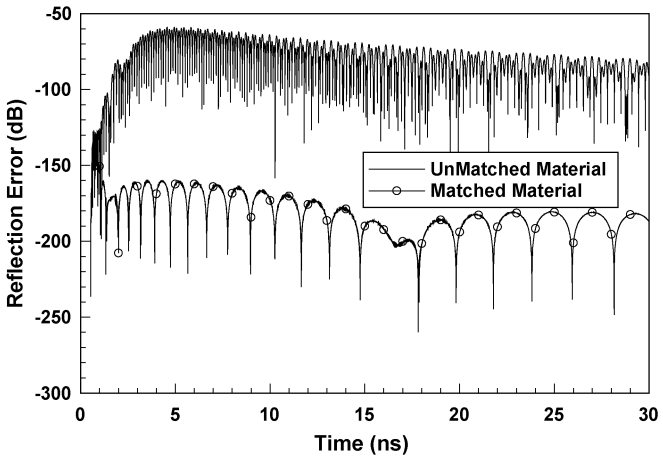

Fig. 1. Reflection error as a function of time.

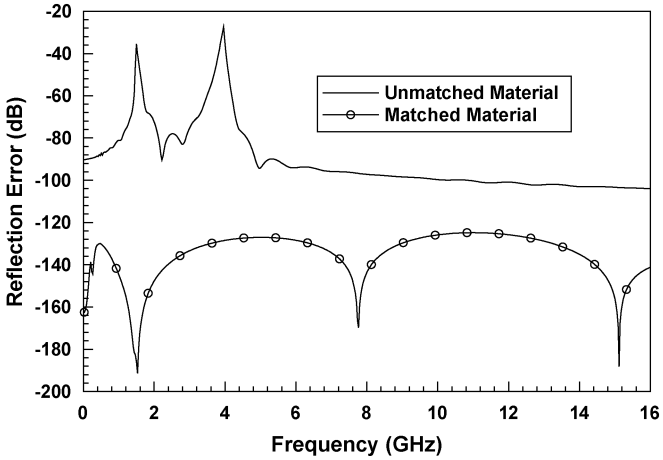

Fig. 2. Reflection error as a function of frequency.

V. Conclusion

In this letter, the uniaxial PML is extended to truncate the boundary of left-handed material, with negative permittivity and permeability. The effectiveness of the PML is demonstrated by numerical examples.

Appendix

The coefficients a_m and b_m in (7) are

$$a_1 = \frac{\left[\varepsilon_0\kappa_z\left(2\omega_{pe}^2\Delta t^2 - 8\right) + 2\sigma_z\Gamma_e\Delta t^2\right]}{A}$$

$$a_2 = \frac{\left[\varepsilon_0\kappa_z\left(\omega_{pe}^2\Delta t^2 - 2\Gamma_e\Delta t + 4\right) + \sigma_z\Gamma_e\Delta t^2 - 2\sigma_z\Delta t\right]}{A}$$

$$b_0 = \frac{(4 + 2\Gamma_e\Delta t)}{A}, \quad b_1 = -\frac{8}{A}, \quad b_2 = \frac{(4 - 2\Gamma_e\Delta t)}{A}$$

where

$$A = \varepsilon_0\kappa_z\left(\omega_{pe}^2\Delta t^2 + 2\Gamma_e\Delta t + 4\right) + \sigma_z\Gamma_e\Delta t^2 + 2\sigma_z\Delta t.$$

The coefficients c_m and d_m in (8) are

$$\begin{aligned}
c_1 &= 4/C\big[\varepsilon_0\mu_0\kappa_z\big(\omega_{pe}^2\omega_{pm}^2\Delta t^4+\Gamma_e\omega_{pm}^2\Delta t^3+\Gamma_m\omega_{pe}^2\Delta t^3 \\
&\qquad -4\Gamma_m\Delta t-4\Gamma_e\Delta t-16\big) \\
&\quad + \mu_0\sigma_z\Delta t\big(\Gamma_e\omega_{pm}^2\Delta t^3+\omega_{pm}^2\Delta t^2 \\
&\qquad +\Gamma_e\Gamma_m\Delta t^2-4\big)\big] \\
c_2 &= 1/C\big[\varepsilon_0\mu_0\kappa_z\big(6\omega_{pe}^2\omega_{pm}^2\Delta t^4-8\omega_{pe}^2\Delta t^2-8\omega_{pm}^2\Delta t^2 \\
&\qquad -8\Gamma_e\Gamma_m\Delta t^2+96\big) \\
&\quad +\mu_0\sigma_z\Delta t^2\big(6\Gamma_e\omega_{pm}^2\Delta t^2-8\Gamma_m-8\Gamma_e\big)\big] \\
c_3 &= 4/C\big[\varepsilon_0\mu_0\kappa_z\big(\omega_{pe}^2\omega_{pm}^2\Delta t^4-\Gamma_e\omega_{pm}^2\Delta t^3-\Gamma_m\omega_{pe}^2\Delta t^3 \\
&\qquad +4\Gamma_e\Delta t+4\Gamma_m\Delta t-16\big) \\
&\quad + \mu_0\sigma_z\Delta t\big(\Gamma_e\omega_{pm}^2\Delta t^3-\omega_{pm}^2\Delta t^2 \\
&\qquad -\Gamma_e\Gamma_m\Delta t^2+4\big)\big] \\
c_4 &= 1/C\big[\varepsilon_0\mu_0\kappa_z\big(\omega_{pe}^2\omega_{pm}^2\Delta t^4-2\omega_{pe}^2\Gamma_m\Delta t^3-2\omega_{pm}^2\Gamma_e\Delta t^3 \\
&\qquad +4\omega_{pe}^2\Delta t^2+4\omega_{pm}^2\Delta t^2+4\Gamma_e\Gamma_m\Delta t^2 \\
&\qquad -8\Gamma_e\Delta t-8\Gamma_m\Delta t+16\big) \\
&\quad \times \mu_0\sigma_z\Delta t\big(\Gamma_e\omega_{pm}^2\Delta t^3-2\omega_{pm}^2\Delta t^2-2\Gamma_e\Gamma_m\Delta t^2 \\
&\qquad +4\Gamma_e\Delta t+4\Gamma_m\Delta t-8\big)\big] \\
d_0 &= 2\varepsilon_0/C\big[\omega_{pe}^2\Gamma_m\Delta t^3+2\omega_{pe}^2\Delta t^2+2\Gamma_e\Gamma_m\Delta t^2 \\
&\qquad +4(\Gamma_e+\Gamma_m)\Delta t+8\big] \\
d_1 &= 4\varepsilon_0/C\big(\omega_{pe}^2\Gamma_m\Delta t^3-4\Gamma_e\Delta t-4\Gamma_m\Delta t-16\big) \\
d_2 &= -8\varepsilon_0/C\big(\Gamma_m\Gamma_e\Delta t^2+\omega_{pe}^2\Delta t^2-12\big) \\
d_3 &= -4\varepsilon_0/C\big(\omega_{pe}^2\Gamma_m\Delta t^3-4\Gamma_e\Delta t-4\Gamma_m\Delta t+16\big) \\
d_4 &= -2\varepsilon_0/C\big(\omega_{pe}^2\Gamma_m\Delta t^3-2\omega_{pe}^2\Delta t^2-2\Gamma_e\Gamma_m\Delta t^2 \\
&\qquad +4\Gamma_e\Delta t+4\Gamma_m\Delta t-8\big)
\end{aligned}$$

where

$$\begin{aligned}
C &= \varepsilon_0\mu_0\kappa_z\left(\omega_{pe}^2\omega_{pm}^2\Delta t^4+2\omega_{pm}^2\Gamma_e\Delta t^3+2\omega_{pe}^2\Gamma_m\Delta t^3\right. \\
&\qquad +4\omega_{pm}^2\Delta t^2+4\Gamma_e\Gamma_m\Delta t^2+4\omega_{pe}^2\Delta t^2 \\
&\qquad \left.+8\Gamma_m\Delta t+8\Gamma_e\Delta t+16\right) \\
&\quad +\mu_0\sigma_z\Delta t\left(\Gamma_e\omega_{pm}^2\Delta t^3+2\omega_{pm}^2\Delta t^2\right. \\
&\qquad \left.+2\Gamma_e\Gamma_m\Delta t^2 4\Gamma_m\Delta t+4\Gamma_e\Delta t+8\right).
\end{aligned}$$

REFERENCES

[1] D. R. Smith and N. Kroll, "Negative refractive index in left-handed materials," *Phys. Rev. Lett.*, vol. 85, no. 14, pp. 2933–2936, Oct. 2000.

[2] J. B. Pendry, "Negative refraction makes a perfect lens," *Phys. Rev. Lett.*, vol. 85, no. 18, pp. 3966–3969, Oct. 2000.

[3] P. M. Valanju, R. M. Walser, and A. P. Valanju, "Wave refraction in negative-index media: always positive and very infomogeneous," *Phys. Rev. Lett.*, vol. 88, no. 18, May 2002.

[4] N. Garcia and M. Nieto-Vesperinas, "Left-handed materials do not make a perfect lens," *Phys. Rev. Lett.*, vol. 88, no. 20, May 2002.

[5] R. W. Ziolkowski, "Wave propagation in media having negative permittivity and permeability," *Phys. Rev. E*, vol. 64, no. 5, Oct. 2001.

[6] S. A. Cummer, "Simulated causal subwavelength focusing by a negative refractive index slab," *Appl. Phys. Lett.*, vol. 82, no. 10, pp. 1503–1505, Mar. 2003.

[7] J. P. Berenger, "A perfectly matched layer for the absorption of electromagnetic waves," *J. Comput. Phys.*, vol. 114, pp. 185–200, Oct. 1994.

[8] Z. S. Sacks, D. M. Kingsland, R. Lee, and J. F. Lee, "A perfectly matched anisotropic absorber for use as an absorbing boundary condition," *IEEE Trans. Antennas Propagat.*, vol. 43, pp. 1460–1463, Dec. 1995.

[9] S. D. Gedney, "An anisotropic perfectly matched layer-absorbing medium for the truncation of FDTD lattices," *IEEE Trans. Antenna Propagat.*, vol. 44, no. 12, pp. 1630–1639, Dec. 1996.

[10] ——, "An anisotropic PML absorbing media for the FDTD simulation of fields in lossy and dispersive media," *Electromagn.*, vol. 16, pp. 399–415, 1996.

[11] D. M. Sullivan, *Electromagnetic Simulation Using the FDTD Method*. Piscataway, NJ: IEEE Press, 2000.